Cell Death & Differentiation (2018) 25:1304–1318
https://doi.org/10.1038/s41418-017-0041-z

Cell Death & Differentiation

ARTICLE

Type I IFN operates pyroptosis and necroptosis during multidrug-resistant *A. baumannii* infection

Yang Li[1] · Xiaomin Guo[1] · Chunmiao Hu[1] · Yan Du[2] · Chuansheng Guo[3] · Di Wang[3] · Weiheng Zhao[4] · Gonghua Huang[4] · Chunliang Li[5] · Qiumin Lu[1] · Ren Lai[1] · Tao Xu[1] · Xiaopeng Qi[1]

Received: 21 June 2017 / Revised: 13 November 2017 / Accepted: 15 November 2017 / Published online: 19 January 2018

Abstract

Multidrug-resistant *Acinetobacter baumannii*, a common pathogen responsible for nosocomial infections, is the main cause for outbreaks of infectious diseases, such as pneumonia, meningitis, and bacteremia, especially among critically ill patients. Epidemic *A. baumannii* is a growing public health concern as it is resistant to all existing antimicrobial agents, thereby necessitating the development of new therapeutic approaches to mount an effective immune response against this bacterial pathogen. In this study, we identified a critical role for type I interferon (IFN) in epigenetic regulation during *A. baumannii* infection and established a central role for it in multiple cell death pathways. *A. baumannii* infection induced mixed cell death constituted of apoptosis, pyroptosis, and necroptosis. Mechanically, *A. baumannii* triggered TRIF-dependent type I IFN production, which in turn induced the expression of genes *Zbp1*, *Mlkl*, *caspase-11*, and *Gsdmd* via KAT2B-mediated and P300-mediated H3K27ac modification, leading to NLRP3 inflammasome activation, and potentially contributed to GSDMD-mediated pyroptosis and MLKL-dependent necroptosis. Our study offers novel insights into the mechanisms of type I IFN and provides potential therapeutic targets for infectious and inflammatory diseases.

Introduction

Acinetobacter baumannii is a rod-shaped, Gram-negative, nosocomial bacterium that generally affects individuals with compromised immune function. Multidrug-resistant (MDR) *A. baumannii* has been recognized as a major global public health threat because it is resistant to all commonly used antibiotics and was listed in the Bad Bugs, No Drugs Campaign by the Infectious Diseases Society of America [1–3]. Thus, it is essential to comprehensively understand the pathogenesis of MDR *A. baumannii* and host immune responses.

Type I interferons (IFNs) are a group of IFN proteins that are critical for calibrating host defense against viral and bacterial infections while attenuating tissue damage and preventing autoimmunity. Canonical type I IFN signaling activates the Janus kinase-signal transducer and activator of transcription (JAK-STAT) pathway, leading to expression of

Edited by A. Oberst

Yang Li and Xiaomin Guo are Co-first author.

Electronic supplementary material The online version of this article (https://doi.org/10.1038/s41418-017-0041-z) contains supplementary material, which is available to authorized users.

✉ Ren Lai
rlai@mail.kiz.ac.cn

✉ Tao Xu
xutao@mail.kiz.ac.cn

✉ Xiaopeng Qi
qixiaopeng@mail.kiz.ac.cn

[1] Key Laboratory of Animal Models and Human Disease Mechanisms of Chinese Academy of Sciences/Key Laboratory of Bioactive Peptides of Yunnan Province, Kunming Institute of Zoology, Chinese Academy of Sciences, 650223 Kunming, Yunnan, China

[2] Department of Clinical Laboratory, The First Affiliated Hospital of Kunming Medical University, 295 Xichang Road, 650032 Kunming, Yunnan, China

[3] Institute of Immunology, Zhejiang University School of Medicine, 310058 Hangzhou, China

[4] Shanghai Institute of Immunology, Institute of Medical Sciences, Shanghai Jiao Tong University School of Medicine, Shanghai, China

[5] Cancer Biology Program, Department of Tumor Cell Biology, St. Jude Children's Research Hospital, Memphis, TN 38105, USA

IFN-stimulated genes (ISGs), including classical antiviral and pro-inflammatory genes [4]. Type I IFNs protect host defense against acute viral infections. However, the role of type I IFNs in bacterial infections remains unclear [5–7]. Mice lacking the type I IFN receptor exhibit increased susceptibility to *Streptococcus pyogenes* and *Helicobacter pylori* infections [8, 9]. In contrast, during *Brucella abortus*, *Francisella novicida*, *Listeria monocytogenes*, *Salmonella* Typhimurium, and *Mycobacterium tuberculosis* infections, type I IFN impairs host control of bacterial growth by modulating distinct cellular processes and immune responses [10–14].

Host cell death is an intrinsic cell defense mechanism during bacterial infection. Recent studies have conclusively demonstrated that the necroptotic and pyroptotic cell death pathways are crucial for the release and action of inflammatory cytokines [15, 16]. Likewise, activation of type I IFN-dependent noncanonical NLRP3 and AIM2 inflammasomes and subsequent pyroptotic cell death play critical roles in host defense against *Escherichia coli* and *F. novicida* infection, respectively [17, 18]. In addition, type I IFN also modulates apoptosis and necroptosis in response to *L. monocytogenes* and *S.* Typhimurium infection [12, 19]. Despite advances in the study of type I IFN and cell death in infectious diseases, the mechanisms underlying the production of type I IFNs and their function in host defense against MDR bacteria, such as epidemic MDR *A. baumannii* remain to be elucidated.

Herein, we identified a protective role for type I IFNs in host defense against MDR *A. baumannii* infection. *A. baumannii* infection triggered multiple cell death pathways, such as apoptosis and two inflammatory programmed cell death including necroptosis and pyroptosis. Genetic deletion of IFN-alpha receptor (IFNAR)-inhibited TIR domain-containing adapter-inducing IFN-β (TRIF)-mediated activation of NLRP3 inflammasome, pyroptosis, and necroptosis in response to MDR *A. baumannii* infection. Type I IFN epigenetically regulated the expression of key mediators of cell death pathways through modulating the expression of *Kat2b* and *P300*, which are crucial for acetylation of histone H3 Lysine 27 (H3K27Ac). Thus, our study reports a novel mechanism through which type I IFN induces necroptosis and pyroptosis, which provides insight of type I IFN highly relevant to infectious and inflammatory diseases and potential targets for modulating type I IFN signaling during *A. baumannii* infection.

Results

Type I IFN plays protective roles in host defense against A. baumannii infection

The engagement of pathogen-associated molecular patterns derived from extracellular and intracellular bacterial pathogens and various membrane or cytosolic pattern recognition receptors can trigger robust type I IFN production through diverse pathways. During *A. baumannii* infection, the expression of *Ifnb* and inducible gene *Cxcl9*, and genes that are encoding proinflammatory cytokines including *Il1a*, *Il6*, and *Tnfa* were significantly induced in wild-type (WT) primary bone marrow-derived macrophages (BMDMs) but not in *Ifnar*$^{-/-}$ or *Irf3*$^{-/-}$/*Irf7*$^{-/-}$ (*Irf3/7*$^{-/-}$) primary BMDMs (Fig. 1a). Consistently, the production of IFN-β, TNF-α, IL-1α, and IL-6 induced by *A. baumannii* infection was diminished in *Ifnar*$^{-/-}$ and *Irf3*$^{-/-}$/*Irf7*$^{-/-}$ BMDMs (Fig. 1b), indicating that IRF3 and IRF7 play integral roles in the production of type I IFN and cytokines during *A. baumannii* infection. Moreover, *Ifnb* expression was not dependent on IL-1α or IL-1β during *A. baumannii* infection (Supplementary Figure S1). To examine the role of type I IFN in host defense against *A. baumannii* infection, WT mice and mice deficient in type I IFN receptor or IRF3 and IRF7 were intranasally administered with *A. baumannii*, and bacterial burden in the lungs and systemic organs was measured 2 days after infection. Bacterial loads in the lungs and spleens of WT mice were significantly lower than those in *Ifnar*$^{-/-}$ and *Irf3*$^{-/-}$*Irf7*$^{-/-}$ mice, though bacterial loads in the liver were comparable between both groups (Fig. 1c). In line with this data, the disease symptoms of *Ifnar*$^{-/-}$ mice infected with *A. baumannii* were more severe than that of WT mice at 6–10 h after infection (Fig. 1d). These results suggest that type I IFN plays protective roles in host defense against *A. baumannii* infection.

High immune cell infiltration and inflammatory cytokine production can reduce bacterial burden. Thus, we analyzed immune cell infiltration in the lungs of mice. Immune cell infiltration and airway smooth muscle hypertrophy were significantly higher in lungs of WT mice than in lungs of *Ifnar*$^{-/-}$ after infection (Fig. 1e). In contrast, bacterial burden was higher in the airways of lungs of *Ifnar*$^{-/-}$ mice than those of WT mice (Fig. 1e). Consistent with the observation of more inflammation in WT mice than in *Ifnar*$^{-/-}$ mice, expression of *Ifnb*, *Cxcl9*, and pro-inflammatory cytokine genes, such as *Il6*, *Tnfa*, *Il1a*, and *Cxcl1* was significantly higher in lungs of WT mice than those of *Ifnar*$^{-/-}$ mice after infection (Fig. 1f). In addition, the production of IFN-β, TNF-α, IL-1α, and IL-6 in mice induced by *A. baumannii* infection was substantially reduced in the absence of IFNAR (Fig. 1g). Taken together, these findings indicate that the type I IFN-mediated inflammatory response positively affects host defense against *A. baumannii* infection.

A. baumannii infection induces activation of multiple cell death pathways

Cell death pathways, in particular the necroptotic and pyroptotic cell death are crucial for the release and action of

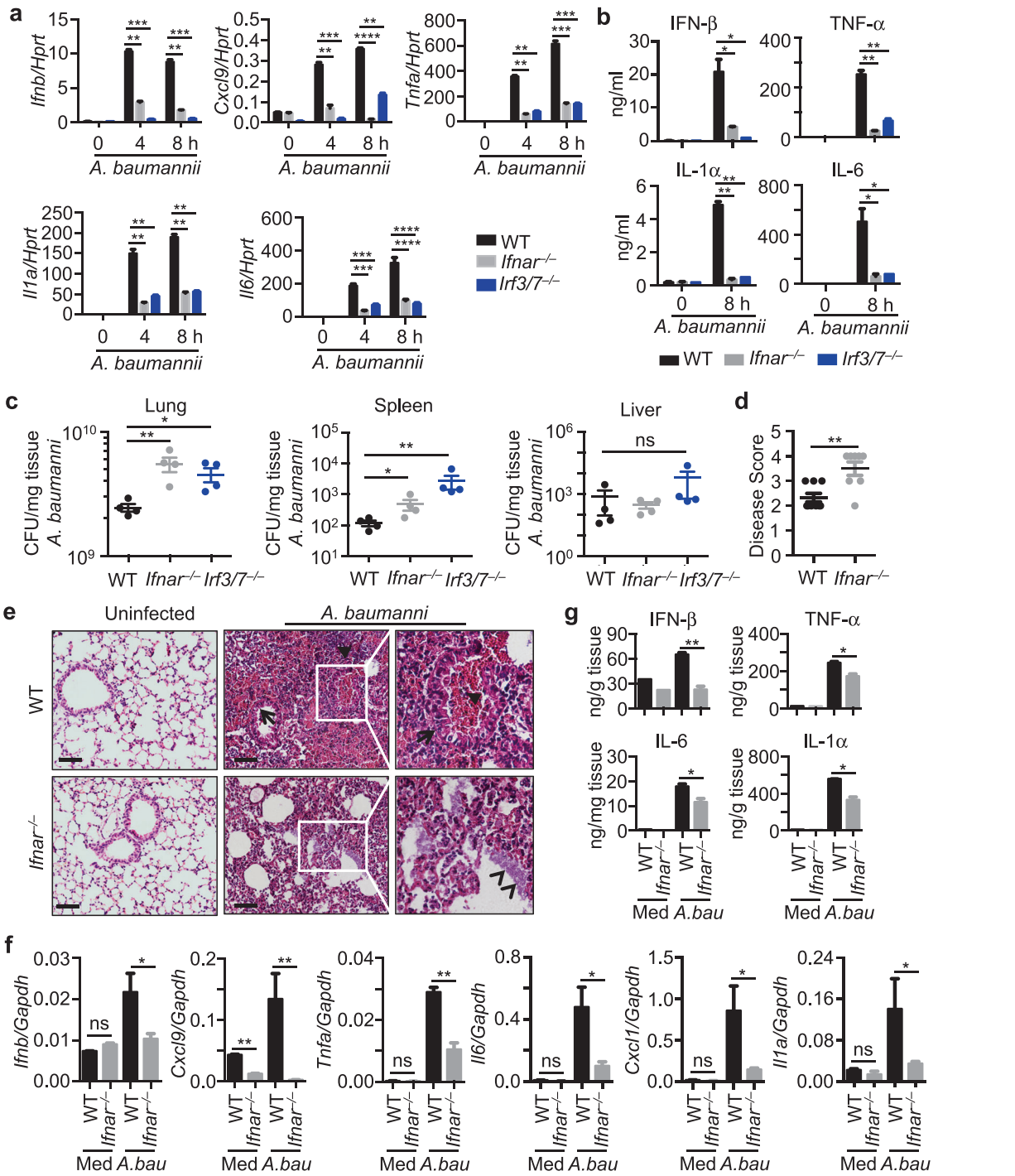

Fig. 1 *Ifnar*$^{-/-}$ mice were more susceptible to *A. baumannii* infection. **a** The expression of *Ifnb*, *Cxcl9*, *Tnfa, Il1a,* and *Il6* was analyzed in WT, *Irf3*$^{-/-}$*/Irf7*$^{-/-}$ (*Irf3/7*$^{-/-}$) and *Ifnar*$^{-/-}$ BMDMs infected with 50 MOI of *A. baumannii* for the indicated times by quantitative RT-PCR. **b** The production of IFN-β, TNF-α, IL-1α, and IL-6 in WT, *Irf3/7*$^{-/-}$, and *Ifnar*$^{-/-}$ BMDMs was measured by ELISA. **c** WT, *Irf3/7*$^{-/-}$, and *Ifnar*$^{-/-}$ mice were intranasally infected with 3.0×10^8 CFU of *A. baumannii*. Bacterial burden in lung, spleen, and liver on day 2 after infection was measured. Each symbol indicates an individual mouse. **d** WT and *Ifnar*$^{-/-}$ mice were intranasally infected with 1.5×10^9 CFU of *A. baumannii* and disease score was recorded 8 h after infection. **e** Representative lung hematoxylin and eosin (H&E) sections from *A. baumannii* infected and uninfected WT and *Ifnar*$^{-/-}$ mice. Arrow and arrowhead indicate thick airway muscle and bacteria, respectively. Triangle indicates immune cell infiltration. **f** The expression of *Ifnb*, *Cxcl9*, *Tnfa*, *Il6*, *Cxcl1*, and *Il1a* was analyzed in WT and *Ifnar*$^{-/-}$ lungs at day 2 after infection and uninfected lungs by quantitative RT-PCR. **g** The production of IFN-β, TNF-α, IL-1α, and IL-6 in WT and *Ifnar*$^{-/-}$ lungs at day 2 after infection and uninfected lungs by ELISA. Data are representative of three independent experiments for **a and b**, and two independent experiments for **c–g**. Scale bars, 50 μm. Data are means ± SEM. $^*P < 0.05$; $^{**}P < 0.01$; $^{***}P < 0.001$; $^{****}P < 0.0001$; ns, not significant

inflammatory cytokines. The maturation of caspase-3 and caspase-1 were key events for inducing apoptosis and pyroptosis, respectively [16, 20]. Necroptosis was mediated by the activation of receptor interacting protein kinase 1 (RIPK1) and RIPK3 upstream of the executor for necroptosis-mixed lineage kinase domain-like protein (MLKL) [21]. To examine which kind of cell death was induced during *A. baumannii* infection, we performed WT BMDMs infected with *A. baumannii* and examined the cell death in the absence or presence of different inhibitors treatments, which can block the various cell death pathways including apoptosis, pyroptosis, and necroptosis. Notably, the level of apoptosis labeled by caspase-3 cleavage induced by *A. baumannii* infection was inhibited by caspase inhibitor zVAD, but not by inhibitors with blocking the activity of RIPK1, RIPK3, MLKL, or caspase-1 (Fig. 2a). *A. baumannii* infection also induced the hallmarks of pyroptosis–caspase-1 activation and the subsequent release of caspase-1 substrate IL-1β, which were inhibited in the presence of caspase-1 inhibitor but not other inhibitors (Fig. 2b, c). To determine whether *A. baumannii* infection can induce necroptosis, we performed flow cytometry analysis using propidium iodide (PI) and annexin V staining, and lactate dehydrogenase (LDH) release analysis for the WT BMDMs infected with *A. baumannii* in the presence of different inhibitors treatments. Strikingly, RIPK1, RIPK3, and MLKL inhibitors reduced the percentage of cell population double positive for PI and annexin V staining compared with control (Fig. 2d, e). Consistently, the cell death reduced by RIPK1, RIPK3, and MLKL inhibitors was also confirmed by LDH release (Fig. 2f). Collectively, these data indicated *A. baumannii* infection triggered mixed cell

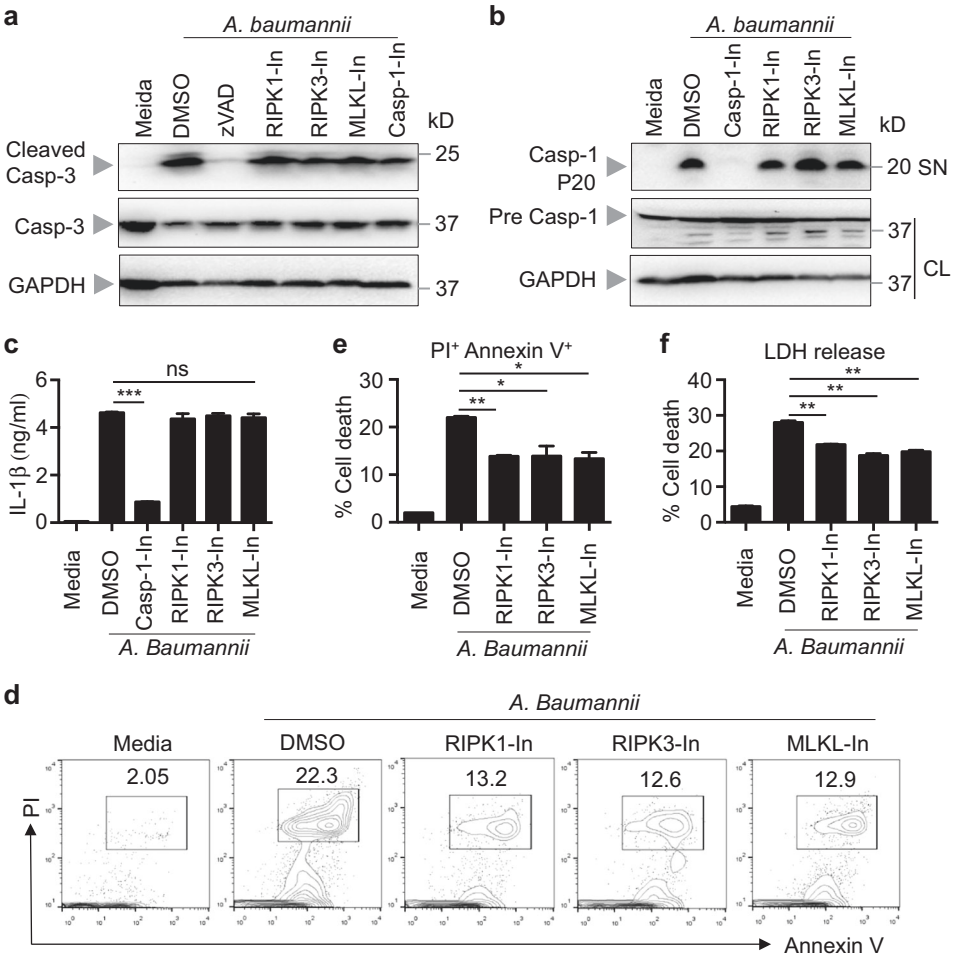

Fig. 2 *A. baumannii* infection-induced apoptosis, necroptosis, and pyroptosis.**a** Immunoblot analysis of caspase-3 preform (Casp-3), and cleaved caspase-3 in WT BMDMs infected with *A. baumannii* (MOI 50) in the presence of zVAD (20 μM), RIPK1 inhibitor (10 μM), RIPK3 inhibitor (20 μM), MLKL inhibitor (20 μM), or caspase-1 inhibitor (25 μM) for 5 h. **b** Immunoblot analysis of caspase-1 preform and cleaved caspase-1 (P20) in WT BMDMs infected with *A. baumannii* (MOI 50) in the presence of caspase-1 inhibitor (25 μM), RIPK1 inhibitor (10 μM), RIPK3 inhibitor (20 μM), or MLKL inhibitor (20 μM) for 12 h. **c** IL-1β ELISA analysis for samples in **b**. **d** Flow cytometry analysis of PI and annexin V staining in WT BMDMs infected with *A. baumannii* (MOI 50) in the presence of RIPK1 inhibitor (10 μM), RIPK3 inhibitor (20 μM), or MLKL inhibitor (20 μM) for 5 h. **e** The quantification analysis of double positive cells with PI and annexin V staining for **d**. **f** LDH release analysis of WT BMDMs infected with *A. baumannii* (MOI 50) in the presence of RIPK1 inhibitor (10 μM), RIPK3 inhibitor (20 μM), or MLKL inhibitor (20 μM) for 5 h. Data are representative of three independent experiments. Data are means ± SEM. $*P < 0.05$; $**P < 0.01$; $***P < 0.001$. SN supernatant, CL cell lysate

death constituted of apoptosis, pyroptosis, and necroptosis. However, which kind of cell death happened first and the connection between these cell death events or whether all these different cell death pathways were triggered in one and the same cell by *A. baumannii* infection need to be examined by single-cell analysis.

Apoptosis, necroptosis, and pyroptosis are attenuated in the absence of IFNAR during A. baumannii infection

To examine whether the pyroptosis mediated by inflammasome activation was affected by IFNAR during *A. baumannii* infection, we analyzed caspase-1 activation in infected liver tissue samples of WT and *Ifnar*$^{-/-}$ mice. Activation of caspase-1 was impaired in the absence of IFNAR after 2 days of infection (Fig. 3a). Consistent with this data, two hallmarks of pyroptosis—the activation of caspase-1 and the subsequent release of caspase-1 substrate IL-1β—were lower in *Ifnar*$^{-/-}$ BMDMs than those in WT BMDMs during *A. baumannii* infection (Fig. 3b). Genes stimulated by type I IFN have been reported to be mediators of apoptosis, having pleiotropic anti-tumor and anti-viral effects [22]. In line with this finding, we observed that activation of apoptotic caspase-3 was abolished in *Ifnar*$^{-/-}$ mice and BMDMs in response to infection (Fig. 3a, b). WT and *Ifnar*$^{-/-}$ BMDMs were infected with *A. baumannii* and necroptosis was determined by flow cytometry using PI and annexin V staining. Strikingly, the percentage of cell populations double positive for PI and annexin V staining in *Ifnar*$^{-/-}$ BMDMs was significantly lower than that in WT BMDMs during *A. baumannii* infection (Fig. 3c), indicating reduced necroptosis in *Ifnar*$^{-/-}$ BMDMs. In line with this, the LDH release and the phosphorylation of MLKL induced by *A. baumannii* infection were also impaired in *Ifnar*$^{-/-}$ BMDMs (Fig. 3d, e). However, quantification of autophagy by western blotting using anti-LC3 antibody and of lysosomal biogenesis using anti-TFEB antibody revealed that both autophagy and lysosomal biogenesis did not change substantially in the absence of IFNAR in either liver tissue (Supplementary Figure S2a) or BMDMs (Supplementary Figure S2b) during *A. baumannii* infection, suggesting that type I IFN-mediated cell death is not a feedback from autophagy pathway. Taken together, our results indicate that type I IFN plays critical roles in the host cell death induced by *A. baumannii* infection, most likely by directly influencing key mediators of cell death pathways.

A. baumannii infection induces TRIF-IFN-I-mediated activation of NLRP3 inflammasome

Inflammasome is a key component of cytosolic surveillance during bacterial infection. Type I IFN is required for activation of AIM2 and NLRP3 inflammasomes induced by *F. novicida* and *E. coli* infection [17, 18, 23]. Furthermore, type I IFN-mediated activation of NLRP3 inflammasome is dependent on TRIF, whereas activation of AIM2 inflammasome is dependent on the cyclic GMP–AMP synthase–STING axis [18, 24, 25]. Thus, we investigated whether activation of AIM2 or NLRP3 inflammasome is triggered by *A. baumannii* infection. WT and *Trif*$^{-/-}$ BMDMs were infected with *A. baumannii*, and the expression of type I IFN was analyzed. Notably, the expression of *Ifnb* and *Cxcl9* was completely dependent on TRIF, whereas that of *Tnfa* and *Il1a* was partially dependent on TRIF during *A. baumannii* infection (Fig. 4a). In line with this data, the production of IFN-β, TNF-α, IL-1α, and IL-6 was impaired in *Trif*$^{-/-}$ BMDMs compared with WT BMDMs during *A. baumannii* infection (Fig. 4b). Of note, Western blot using anti-caspase-1 antibody and ELISA measurement of IL-1β secretion revealed that TRIF was required for inflammasome activation induced by *A. baumannii* (Fig. 4c). Consistent with a very recent report [26], caspase-1 activation and IL-1β secretion were completely dependent on NLRP3 inflammasome in response to *A. baumannii* infection (Fig. 4d). In contrast, caspase-1 activation and IL-1β secretion were comparable between WT and *Aim2*$^{-/-}$ BMDMs (Fig. 4e). Taken together, these results indicate that the TRIF–IFN-I–NLRP3 axis is essential for inflammasome activation in response to *A. baumannii* infection.

Type I IFN controls the transcription of key mediators of necroptosis and pyroptosis pathways

In addition to its well-described role in the apoptotic cell death pathway [22], type I IFN mediates necroptosis by regulating the activity of RIPK3 upstream of the executor for necroptosis-MLKL during bacterial infection; however, the direct interaction between IFNAR and RIPK3 has not been confirmed [12, 21]. Z DNA-binding protein 1 (ZBP1, also called DAI/DLM-1), which was initially recognized as a cytosolic DNA sensor that increases DNA-mediated induction of type I IFN [27], was recently identified as a key mediator of the necroptosis pathway by preventing RIPK1 from RIPK3-MLKL-dependent necroptosis during development, skin inflammation, and certain viral infections [28–31]. However, the upstream signal that drives ZBP1 activation and the ZBP1–RIPK3 interaction remains unclear [31]. Pyroptosis, another form of inflammatory programmed necrotic cell death, was recently defined mediated by gasdermin family members. Gasdermin D (GSDMD) functions downstream of caspases-1 and caspases-11 to execute pyroptosis through pore formation on the membrane [32–35].

It is not known whether type I IFN also controls necroptosis and pyroptosis through additional mechanisms

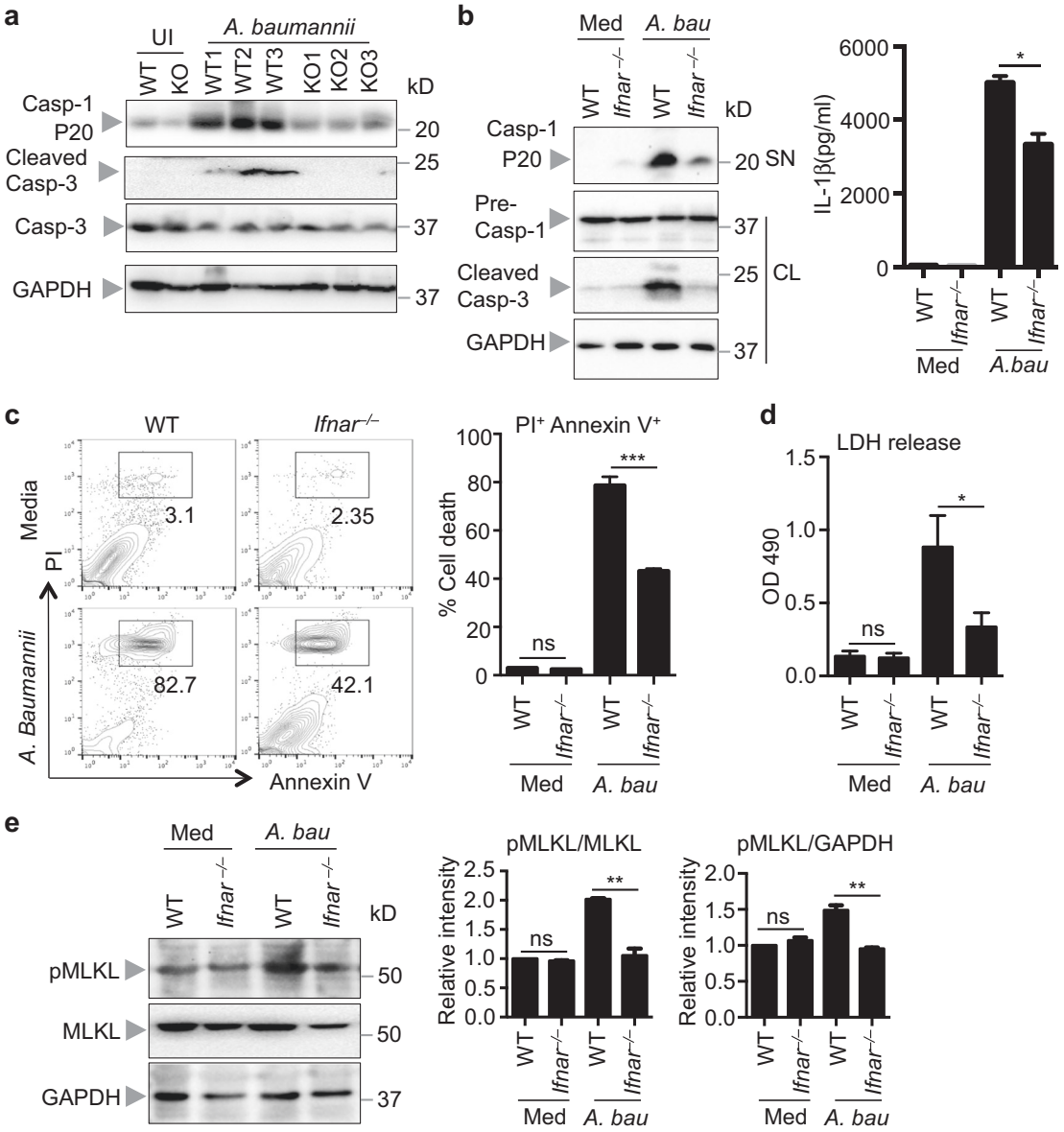

Fig. 3 Cell death was reduced in the absence of Type I IFN signaling in response to *A. baumannii* infection.**a** Liver tissue samples from WT and *Ifnar*$^{-/-}$ mice 2 days after infection with *A. baumannii* were homogenized, and lysates were analyzed for caspase-1 (Casp-1 P20) and caspase-3 (cleaved Casp-3) activation by immunoblot analysis. **b** Immunoblot analysis of caspase-1 preform, its subunit P20 and cleaved caspase-3, and analysis of IL-β release in WT and *Ifnar*$^{-/-}$ BMDMs infected with *A. baumannii* (MOI 50) for 12 h. **c** Flow cytometry analysis of PI and annexin V staining in WT and *Ifnar*$^{-/-}$ BMDMs infected with *A. baumannii* (MOI 50) for 8 h. **d** LDH release analysis of WT and *Ifnar*$^{-/-}$ BMDMs infected with *A. baumannii* (MOI 50) for 8 h. **e** Immunoblot analysis of pMLKL and total MLKL in WT and *Ifnar*$^{-/-}$ BMDMs infected with *A. baumannii* (MOI 50) for 5 h. Data are representative of three independent experiments and are means ± SEM. $*P < 0.05$; $**P < 0.01$; $***P < 0.001$; ns not significant. Med uninfected, *A. bau A. baumannii* infected, SN supernatant, CL cell lysate

in response to *A. baumannii* infection. To determine this, we performed qPCR analysis for key mediators of the necroptosis and pyroptosis in infected liver samples from WT and *Ifnar*$^{-/-}$ mice. Interestingly, expression of *Zbp1*, *Mlkl*, *caspase-11*, and *Gsdmd* but not of *Nlrp3* was markedly lower in samples from infected *Ifnar*$^{-/-}$ mice than those from WT mice (Fig. 5a). To confirm this result, we analyzed the expression of these genes in primary BMDMs. Expression of *Zbp1*, *Mlkl*, *caspase-11*, and *Gsdmd* induced by *A. baumannii* infection was abolished in both *Ifnar*$^{-/-}$ and *Irf3*$^{-/-}$/*Irf7*$^{-/-}$ BMDMs (Fig. 5b). *Zbp1* and *caspase-11* promoters harbor the classical IFN-stimulated response element (ISRE) and are recognized as ISGs [18, 29, 36]. The simultaneously impaired expression of *Zbp1*, *Mlkl*, *caspase-11*, and *Gsdmd* in the lack of type I IFN signaling response to *A. baumannii* infection suggests that type I IFN

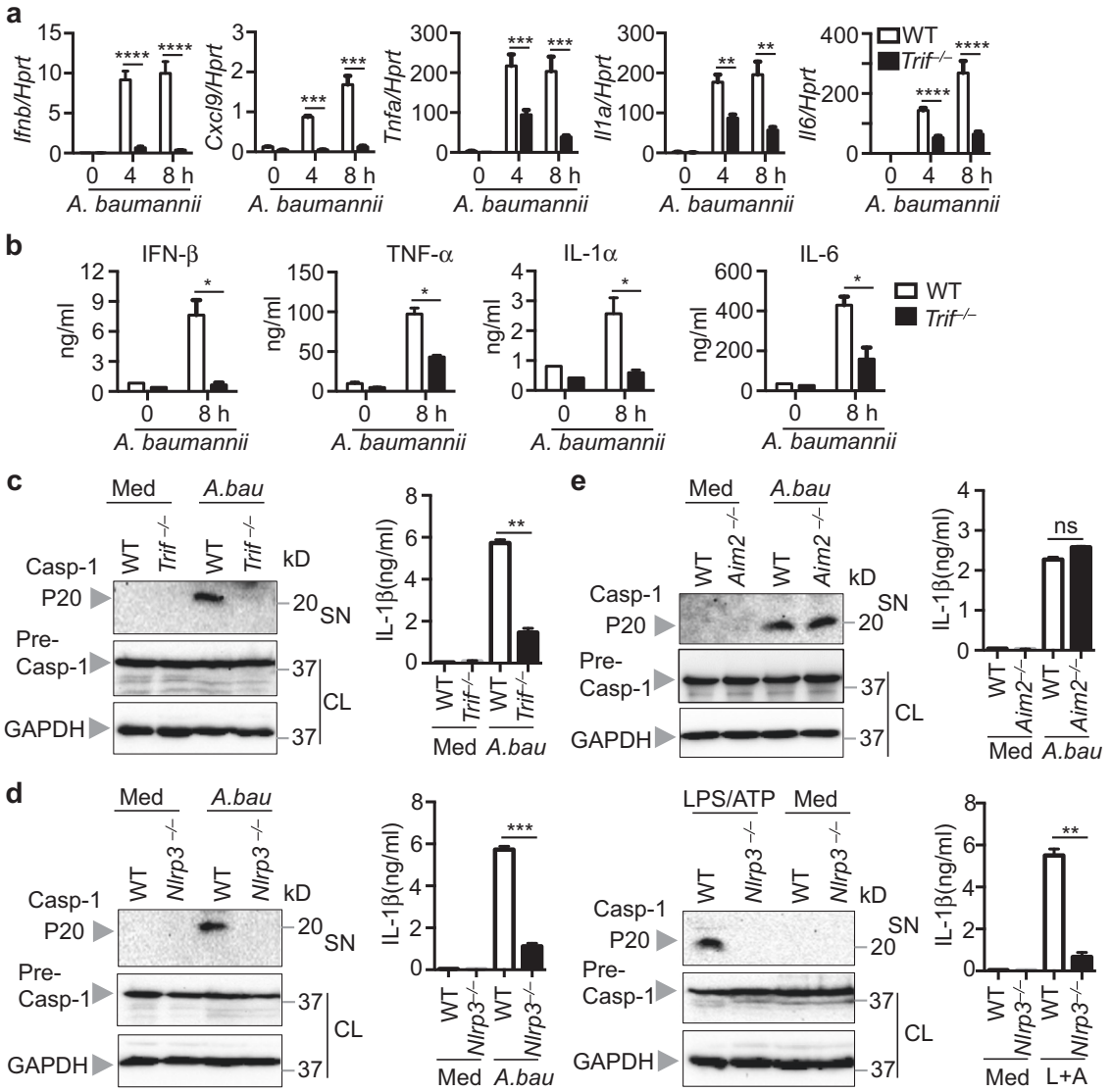

Fig. 4 TRIF–IFN-I axis mediated NLRP3 inflammasome activation response to *A. baumannii* infection.**a** The gene expression of *Ifnb*, *Cxcl9*, *Tnfa*, *Il1a*, and *Il6* was analyzed in WT and *Trif*$^{-/-}$ BMDMs infected with *A. baumannii* for the indicated times by quantitative RT-PCR. **b** The production of IFN-β, TNF-α, IL-1α, and IL-6 in WT and *Trif*$^{-/-}$ BMDMs infected with *A. baumannii* for the indicated times by ELISA. **c** Immunoblot analysis of caspase-1 (Casp-1) and its subunit P20 and analysis of IL-1β release in WT and *Trif*$^{-/-}$ BMDMs infected with *A. baumannii* (MOI 50) for 12 h. **d** Immunoblot analysis of caspase-1 (Casp-1) and its subunit P20 and analysis of IL-1β release in WT and *Nlrp3*$^{-/-}$ BMDMs infected with *A. baumannii* (MOI 50) for 12 h (left) and stimulated with LPS and ATP for 4 h (right). **e** Immunoblot analysis of caspase-1 (Casp-1) and its subunit P20 and analysis of IL-1β release in WT and *Aim2*$^{-/-}$ BMDMs infected with *A. baumannii* (MOI 50) for 12 h. Data are representative of three independent experiments and are means ± SEM. *$P < 0.05$; **$P < 0.01$; ***$P < 0.001$; ****$P < 0.0001$; ns not significant. Med uninfected, *A. bau A. baumannii* infected, SN supernatant, CL cell lysate, L + A LPS and ATP treatment

mediates gene expression through additional mechanisms besides activating ISRE-harboring or GAS-harboring genes.

IFNAR-mediated histone modifications modulates the expression of Zbp1, Mlkl, caspase-11, and Gsdmd

Bacterial infection can regulate host gene expression through epigenetic mechanisms [37]. Histone acetylation or deacetylation is an important chromatin modification induced by the activation of host cell signaling triggered by bacterial components. However, little is known about how signaling cascades in host cells modulate the expression of immunologically relevant genes via epigenetic pathways during pathogenic infection. Two histone modification marks, H3K27ac and H3K4me3, are generally positively associated with gene activation, and H3K27ac appears to be the most dynamic mark in response to external stimuli [38].

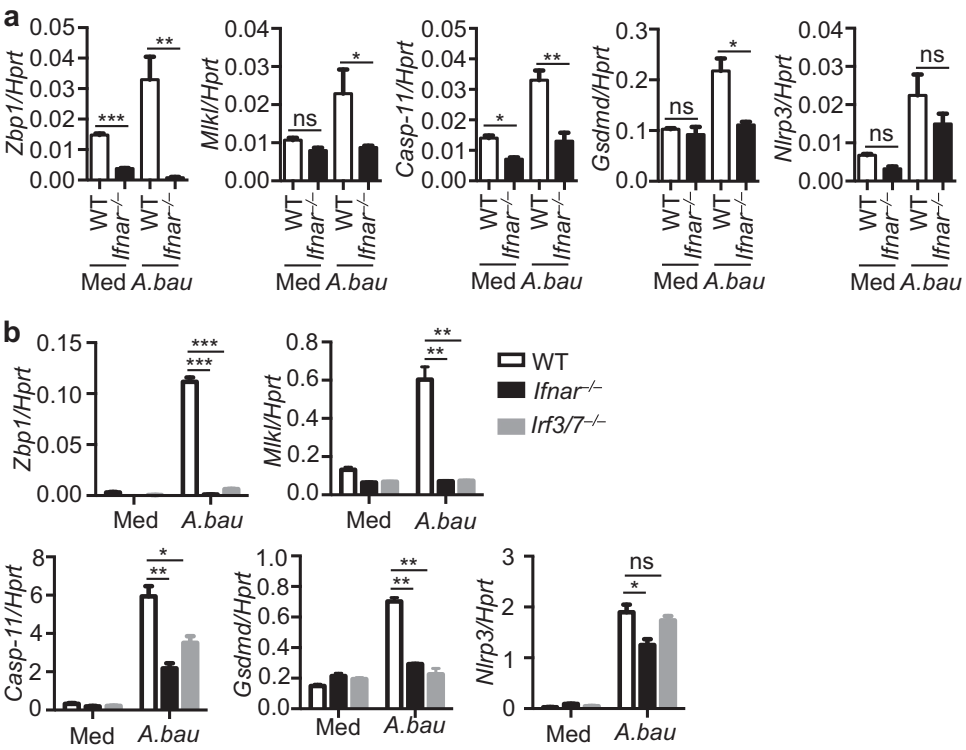

Fig. 5 The expression of key mediators of necroptosis and pyroptosis was reduced in the absence of IFNAR during *Abaumannii* infection. **a** The expression of *Zbp1*, *Mlkl*, *caspase-11*, *Gsdmd*, and *Nlrp3* was analyzed in WT and *Ifnar*$^{-/-}$ livers at day 2 after infection and uninfected livers by quantitative RT-PCR. **b** The expression of *Zbp1*, *Mlkl*, *caspase-11*, *Gsdmd*, and *Nlrp3* was analyzed in WT, *Irf3*$^{-/-}$*Irf7*$^{-/-}$ (*Irf3/7*$^{-/-}$), and *Ifnar*$^{-/-}$ BMDMs infected with *A. baumannii*. Data are representative of two independent experiments for **a**, and three independent experiments for **b**. Data are means ± SEM. *$P < 0.05$; **$P < 0.01$; ***$P < 0.001$; ns not significant. Med uninfected, *A. bau A. baumannii* infected

The level of H3K27ac in WT BMDMs was increased during *A. baumannii* infection, whereas IFNAR deficiency diminished the induction of H3K27ac triggered by *A. baumannii* infection (Fig. 6a). In contrast, the level of H3K4me3 was comparable between WT and *Ifnar*$^{-/-}$ BMDMs, and *A. baumannii* infection did not substantially affect the level of H3K4me3 in WT or *Ifnar*$^{-/-}$ BMDMs (Fig. 6a). To examine whether the induced expression of *Zbp1*, *Mlkl*, *caspase-11*, and *Gsdmd* by type I IFN during *A. baumannii* infection was due to histone modification, we performed chromatin immunoprecipitation (ChIP) coupled with qPCR (ChIP–qPCR) analysis for H3K27ac and H3K4me3 in normal and infected WT and *Ifnar*$^{-/-}$ BMDMs. Based on the ENCODE data crossing different mouse cell lines and tissues [39], ChIP-sequencing signal-rich regions in *Zbp1*, *Mlkl*, *caspase-11*, and *Gsdmd* promoters were selected for ChIP-qPCR analysis (Fig. 6b; and Supplementary Figures S3–S6). Remarkably, ChIP-qPCR revealed that the occupancy of H3K27ac on *Zbp1* and *caspase-11* promoters increased in WT BMDMs but decreased in *Ifnar*$^{-/-}$ BMDMs in response to *A. baumannii* infection (Fig. 6c). In contrast, *A. baumannii* infection did not substantially affect the occupancy of H3K27ac on the *Mlkl* or *Gsdmd* promoter in WT BMDMs (Fig. 6c). However, the occupancy of H3K27ac on *Mlkl* and *Gsdmd* promoters in *Ifnar*$^{-/-}$ BMDMs was markedly reduced during infection (Fig. 6c). Overall, *A. baumannii* infection led to reduced occupancy of H3K27ac on *Zbp1*, *Mlkl*, *caspase-11*, and *Gsdmd* promoters in *Ifnar*$^{-/-}$ BMDMs. Compared with H3K27ac, the binding of H3K4me3 to *Zbp1*, *Mlkl*, *caspase-11*, and *Gsdmd* promoters was largely constant in WT BMDMs, whereas the occupancy of H3K4me3 on *Zbp1*, *Mlkl*, *caspase-11*, and *Gsdmd* promoters was significantly decreased in *Ifnar*$^{-/-}$ BMDMs after *A. baumannii* infection (Fig. 6c). Whereas the increased occupancy of H3K27ac on *caspase-11* promoter and increased occupancy of H3K4me3 on *Mlkl*, *caspase-11*, and *Gsdmd* promoters in uninfected *Ifnar*$^{-/-}$ BMDMs compared with WT BMDMs were observed, the ratio analysis of the occupancy of H3K27ac and H3K4me3 in *Ifnar*$^{-/-}$ relative to WT BMDMs revealed that type I IFN was essential to maintain or increase the binding of these marks to *Zbp1*, *Mlkl*, *caspase-11*, and *Gsdmd* promoters during *A. baumannii* infection (Fig. 6d). Collectively, these findings indicated that lower expression of *Zbp1*, *Mlkl*, *caspase-11*, and *Gsdmd* in *Ifnar*$^{-/-}$ BMDMs in response to *A. baumannii* infection might be due to decreased occupancy of H3K27ac on their promoters.

KAT2B and P300 are crucial for IFN-I-induced cell death during A. baumannii infection

H3K27ac levels are mainly maintained through promotion by acetyltransferases and inhibition by polycomb repressive complex 2 (PRC2), which contribute to chromatin compaction and catalyzes the methylation of histone H3K27 [40–42]. Furthermore, histone demethylase UTX and chromatin remodeler BRM bind to acetyltransferase CBP to

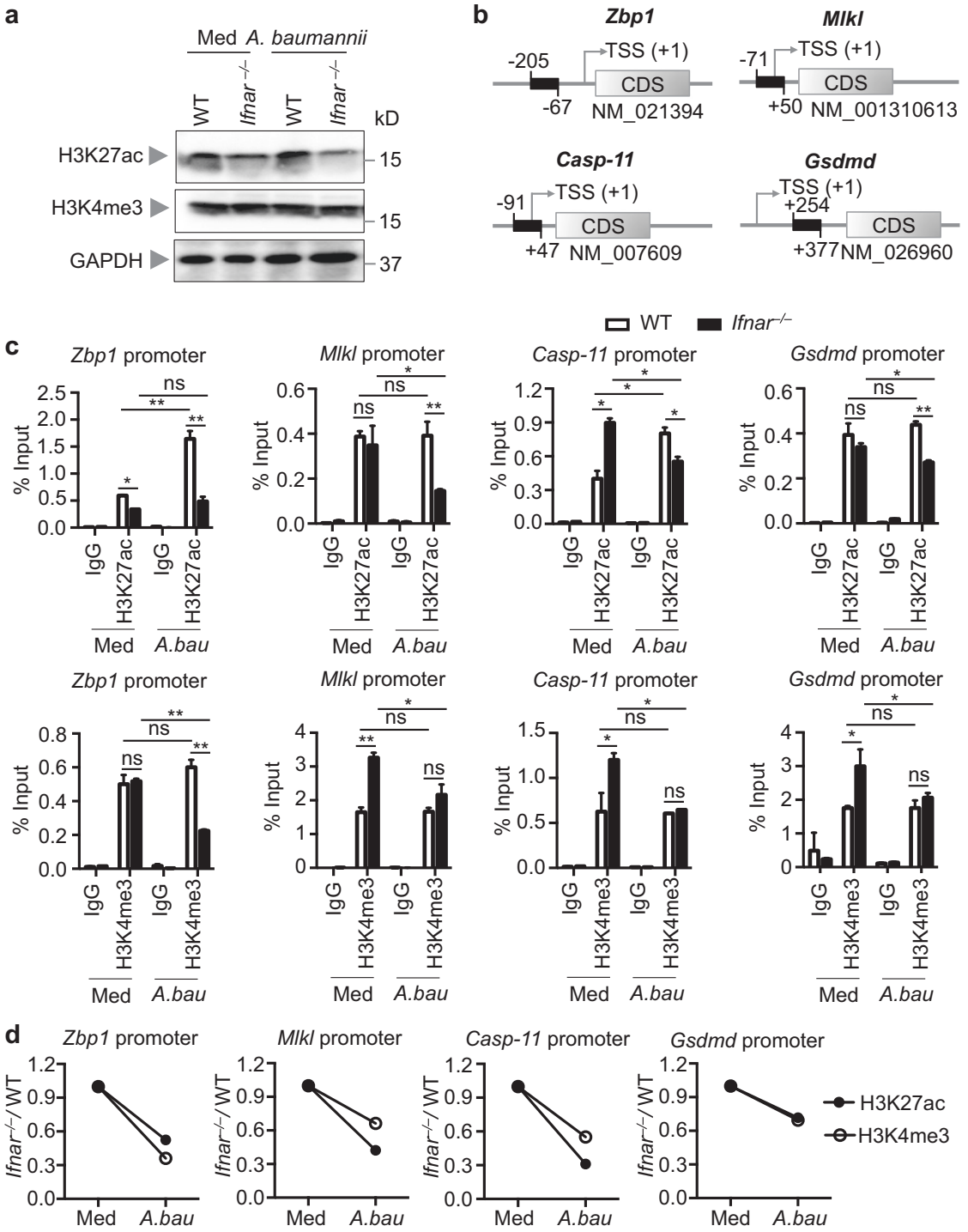

Fig. 6 IFNAR modulated the modification of H3K27ac and H3K4me3 in the promoters of *Zbp1*, *Mlkl*, *caspase-11,* and *Gsdmd* genes.**a** Immunoblot analysis of H3K27ac and H3K4me3 in WT and *Ifnar*$^{-/-}$ BMDMs infected with *A. baumannii* (MOI 50) for 6 h. **b** The promoter regions for ChIP-qPCR analysis. The labeled black rectangle indicates the promoter region of each gene for PCR analysis. **c** ChIP-qPCR analysis of H3K27ac and H3K4me3 modification in the promoters of *Zbp1*, *Mlkl*, *caspase-11* (*Casp-11*) and *Gsdmd* from uninfected and *A. baumannii* infected WT and *Ifnar*$^{-/-}$ BMDMs. **d** Quantification analysis of H3K27ac and H3K4me3 modification in *Ifnar*$^{-/-}$ vs. WT BMDMs. The relative modification in uninfected BMDMs was normalized to 1. Data are representative of two independent experiments and are means ± SEM. *$P < 0.05$; **$P < 0.01$; ns not significant. Med uninfected, *A.bau A. baumannii* infected

promote acetylates histone H3 lysine 27 and inhibit its trimethylation (H3K27me3) [43]. To define the mechanism by which IFN signaling regulates the occupation of H3K27ac on the promoters of *Zbp1*, *Mlkl*, *caspase-11*, and *Gsdmd* in response to *A. baumannii* infection, we first analyzed the expression of genes that encoding major acetyltransferases including KAT1 (HAT1), KAT2A, KAT2B, KAT3A (CBP), KAT3B (P300), and KAT4 (TAF1); the PRC2 compartments SUZ12, EED, and EZH2; and CBP-binding proteins BRM and UTX. Of note, the expression of encoding acetyltransferase genes *Hat1*, *Kat2b*, and *P300* was induced in WT BMDMs by *A. baumannii* infection and the induction was diminished in *Ifnar*$^{-/-}$ and *Irf3*$^{-/-}$/*Irf7*$^{-/-}$BMDMs (Fig. 7a). Importantly, we did not observe similar pattern for the expression of *Kat2a*, *Taf1*, *Kat3a*, *Suz12*, *Eed*, *Ezh2*, *Brm*, or *Utx* (Supplementary Figure S7). This result suggests HAT1, KAT2B, and P300 might contribute to the type I IFN-dependent H3K27ac modification during *A. baumannii* infection. To further examine which acetyltransferase plays pivotal roles in modulating levels of H3K27ac on the promoters of *Zbp1*, *Mlkl*, *caspase-11*, and *Gsdmd* genes, we performed siRNA knockdown experiments for *Hat1*, *Kat2b*, and *P300*. Remarkably, the induced expression of *Zbp1*, *Mlkl*, *caspase-11*, and *Gsdmd* response to *A. baumannii* infection was significantly impaired in *Kat2b* and *P300* knockdown BMDMs, but not in *Hat1* knockdown BMDMs (Fig. 7b–d). Consistently, the level of cell death measured by LDH release indicated that *Kat2b* and *P300* knockdown significantly reduced the cell death triggered by *A. baumannii* infection (Fig. 7e). Collectively, these results indicate type I IFN-dependent KAT2B and P300 contribute to the occupation of H3K27ac on the promoters of *Zbp1*, *Mlkl*, *caspase-11*, and *Gsdmd*, which in turn potentially contributes to their increased expression and cell death activation during *A. baumannii* infection.

Discussion

Host cell death is a double-edged sword for the survival of host and pathogenic bacteria. During bacterial infection, programmed cell death plays defensive roles, such as eliminating pathogens and promoting the secretion of inflammatory cytokines and alarm signals to activate host immune response. The understanding of inflammatory cell death pathways, in particular necroptosis and pyroptosis, has rapidly advanced over recent years. For example, it has been reported that ZBP1 mediates the activation of RIPK3-MLKL-mediated necroptosis, which plays critical roles in host cell necroptosis during development, inflammation, and IAV infection [29–31]. The protein encoded by *Gsdmd* gene was recently identified as the downstream target of caspases-1 and caspases-11, the maturation of which contributes to inflammasome-mediated pyroptosis [32, 33, 44]. Type I IFNs have been established as powerful immunomodulatory and antiviral cytokines, but their function in cell death is not well studied. Our study reveals that type I IFN-dependent cell death plays protective roles in host defense against *A. baumannii* infection. IFNAR deficiency protected cells from necroptosis and pyroptosis through impaired activation of NLRP3 inflammasome and reduced expression of key mediators of cell death pathways in response to *A. baumannii* infection (Supplementary Figure S8).

Consistent with a previous study reporting TRIF-IFNAR-caspase-11 pathway-mediated activation of NLRP3 inflammasome induced by *E. coli* infection [18], we found that TRIF was required for type I IFN production and IFNAR for caspase-11 transcription and autoactivation during *A. baumannii* infection. However, the cytosolic DNA-sensing AIM2 inflammasome was not activated in the presence of *A. baumannii*, and the expressions of *Nlrp3* and *Il1b* were not dependent on IFNAR response to *A. baumannii* infection. These findings suggest that IFN-I-mediated caspase-11 is essential for the activation of NLRP3 inflammasome triggered by *A. baumannii* infection. Further, cytoplasmic lipopolysaccharides derived from Gram-negative bacteria bind to caspase-11 and lead to its oligomerization and activation [45, 46]. We show that in addition to caspase-11, *Gsdmd* transcription is dependent on type I IFN signaling. Thus, our study reveals that type I IFN signaling has profound effects on GSDMD-dependent cell death. Whether other components derived from *A. baumannii* or host cell factors contribute to activation of the caspase-11 and NLRP3 inflammasome, and the requirement of type I IFN signaling for *Gsdmd* expression in other settings need further examination.

Previous studies demonstrated that IFN-I signaling is a key inducer of necroptosis. During *Salmonella* infection, host survival was enhanced in the absence of type I IFN signaling, which was attributed to impaired RIPK3-mediated necroptosis in macrophages [12]. Even though the persistent phosphorylation of RIPK3 maintained by the activation of IFN-stimulated gene factor 3 (ISGF3) was identified, the specific IFN-stimulated gene that mediates RIPK3 activation and necroptosis remained unknown [12, 47]. ZBP1 was conclusively established as the central mediator of RIPK3-MLKL-mediated necroptosis through a direct interaction with RIPK3, which led to RIPK3 autophosphorylation and MLKL-dependent necroptosis [30, 31]. Our finding of IFN-I-dependent *Zbp1* expression in response to *A. baumannii* infection offers insights into understanding the mechanism underlying type I IFN-induced necroptosis. *Zbp1* expression was also shown to depend on type I IFN during IAV infection [29], suggesting that type I IFN-ZBP1 axis-mediated RIPK3-MLKL-dependent necroptosis is a common

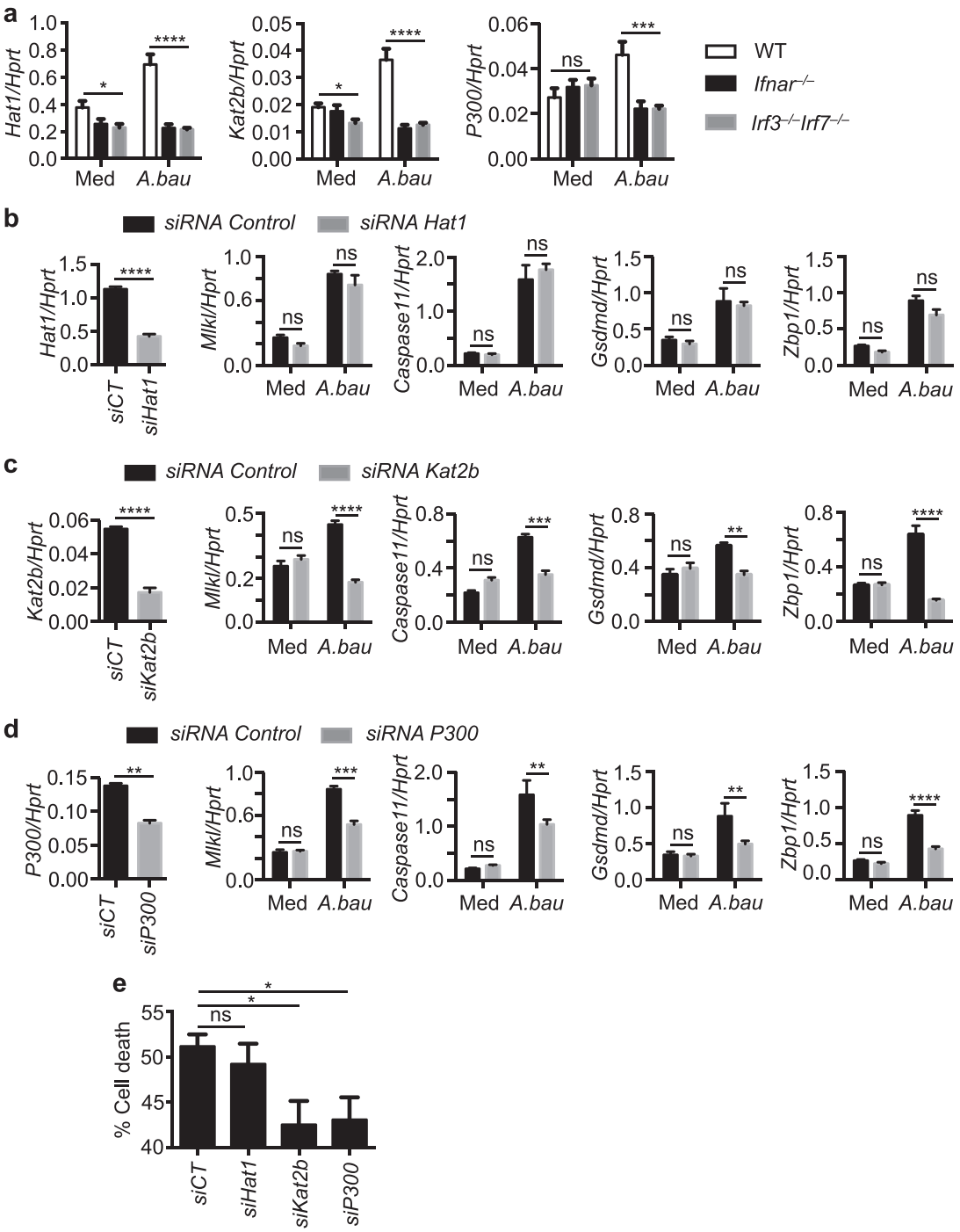

Fig. 7 KAT2B and P300 license type I IFN-dependent expression of *Zbp1*, *Mlkl*, *caspase-11*, and *Gsdmd* upon *A. baumannii* infection. **a** The expression of *Hat1, Kat2b*, and *P300* was analyzed in WT, *Irf3*$^{-/-}$*Irf7*$^{-/-}$, and *Ifnar*$^{-/-}$ BMDMs infected with *A. baumannii* for 6 h. **b–d** The expression of *Mlkl*, *caspase-11*, *Gsdmd,* and *Zbp1* was analyzed in *A. baumannii* infected and uninfected WT BMDMs transfected with *Hat1* siRNA **b**, *Kat2b* siRNA **c**, and *P300* siRNA **d**. **e** LDH release analysis of *A. baumannii* (MOI 50) infected WT BMDMs transfected with *Hat1* siRNA, *Kat2b* siRNA, or *P300* siRNA for 6 h. Data are representative of three independent experiments and are means ± SEM. *$P < 0.05$; **$P < 0.01$; ***$P < 0.001$; ****$P < 0.0001$; ns not significant. Med uninfected, *A. bau A. baumannii* infected, *siCT siRNA control*, *siHat1 siRNA Hat1*, *siKat2b siRNA Kat2b*, *siP300 siRNA P300*

pathway activated during pathogenic infection. Further studies are required to identify the signals that activate ZBP1 during infection.

Recent studies highlight that bacteria can alter epigenetic marks and machineries of host cells to manipulate host cell function, which can either promote host defense or favor

persistent infection. Although type I IFN has been recognized as a powerful cytokine in the host defense mechanism, its role in epigenetic regulation during infection remains ill defined. We observed that the H3K27ac mark was more dynamic than the H3K4me3 mark during *A. baumannii* infection, which is consistent with a previous study reporting that H3K27ac is the most dynamic mark in response to external stimuli in macrophages [38]. Type I IFN contributed to the histone modification change of H3K27ac in response to infection. *Zbp1* and *caspase-11* have been considered as classical ISGs, suggesting that the expressions of *Zbp1* and *caspase-11* are spatiotemporally modulated by type I IFN signaling through both epigenetic regulation and ISGF3.

In summary, we provide an example of epigenetic changes regulating host cell death pathways during bacterial infection. How chromatin changes become localized at specific genomic regions and the fundamental role of type I IFN during bacterial infection are important questions that need to be answered. Our results highlight the importance of histone modifications in programmed cell death pathways during infection and present potential therapeutic targets for controlling bacterial infection and other type I IFN-associated diseases.

Materials and methods

Mice

Ifnar$^{-/-}$, *Irf3*$^{-/-}$*/Irf7*$^{-/-}$, and *Aim2*$^{-/-}$[48] mice were provided by Dr. Feng Shao (National Institute of Biological Sciences, Beijing, China). *Nlrp3*$^{-/-}$ [49] and *Trif*$^{-/-}$[50] mice were generated as described previously. WT and knock out mice were kept in specific pathogen-free conditions within the Animal Resource Center at Kunming Institute of Zoology, Chinese Academy of Sciences. All animal experiments were conducted in accordance with the guidelines and were approved by the Kunming Institute of Zoology, Chinese Academy of Sciences Animal Care and Use Committee.

Bacterial culture and infection of mice

Clinical MDR *A. baumannii* strain (CN40) was isolated from blood of patient in the First Affiliated Hospital of Kunming Medical University (Kunming, China). *A. baumannii* was grown overnight with shaking in brain heart infusion (BHI) medium, sub-cultured for an additional 3–4 h, and resuspended in PBS. Eight to ten weeks old mice were administrated with 3.0×10^8 CFU of *A. baumannii* per mouse through intranasal infection. Mice were weighted and monitored daily over time. Mice were euthanized at day 2 after infection, and liver, spleen, and lung were harvested to determine the bacterial burden. The tissues were homogenized, serially diluted, plated onto BHI agar plates, and incubated overnight at 37 °C. WT and *Ifnar*$^{-/-}$ mice were intranasally infected with 1.5×10^9 CFU of *A. baumannii* per mouse, and the disease scores of mice were monitored and recorded between 6 and 10 h after infection with following standard: 0, no abnormal clinical sign; 1, ruffled fur but lively; 2, ruffled fur, moving slowly, down, and sick; 3, ruffled fur, squeezed eye, hunched, hardly moving, and very sick; 4, moribund; and 5, dead.

Bacterial infection of BMDMs and iBMDMs

Bone marrow cells (BM) from WT and knock out mice were cultured in L929 cell conditioned DMEM supplemented with 10% PBS, 1% non-essential amino acids, and 1% penicillin–streptomycin for 5 days to generate BMDMs. Immortalized BM-derived cells (iBMDMs) from WT, *Il1a*$^{-/-}$, and *Il1b*$^{-/-}$ mice were used for infection. Cells were seeded in 12-well plates (1 million cells per well) and incubated overnight. The next day, cells were washed and supplied with fresh media without antibiotics. Cells were infected with *A. baumannii* for the indicated times. Cells were lysed in radioimmunoprecipitation assay buffer with protease and phosphatase inhibitors (Biotool) for immunoblot analysis.

Preparation of lung sample for HE staining

The superior lobes of the right lungs were fixed in 10% formalin, and 5-mm sections were stained with hematoxylin and eosin and examined.

Immunoblot analysis and antibodies

Samples were separated by 12% SDS-PAGE and followed by electrophoretic transfer to polyvinylidene fluoride membranes, membranes were blocked and incubated with primary antibodies as described previously [20]. The following primary antibodies were used: anti-caspase-1 (AG-20B-0042; Adipogen), anti-LC3B (NB600-1384; Novus Biologicals), anti-caspase-3 (9661s; Cell Signaling Technology), anti-TFEB (A303-673A; Bethyl Laboratories, Inc.), anti-pMLKL (ab196436; abcam), anti-MLKL (ap14272b; abcam), and anti-GAPDH (5174s; Cell Signaling Technology). The secondary antibodies used were HRP-labeled anti-rabbit or anti-mouse antibodies (Cell Signaling Technology).

ChIP analysis

H3K27ac antibody (ab4729) and H3K4me3 antibody (ab8580) were purchased from abcam. ChIP experiments

were carried out by using an EZ ChIP Kit (Millipore, Temecula, CA) as described previously [51]. Briefly, five million cells from each group were cross-linked with 1% formaldehyde, lysed, and sonicated by using Bioruptor Soniction System (UCD-200) to reduce DNA length to an average of 200–700 bp. Sonicated chromatin (supernatant) was diluted in dilution buffer (1:10), and pre-cleared with Protein A Beads at 4 °C for 1 h. Pre-cleared chromatin was incubated with 4 μg of appropriate antibody or IgG control at 4 °C for 12 h. Antibody/chromatin complex was captured by using Protein A beads followed by washing, elution, reverse crosslinking, and DNA isolation. Immunoprecipitated DNA was amplified by qPCR using the primers listed in Table S1.

siRNA transfection

siRNA oligos target to *Hat1* (EMU036281), *Kat2b* (EMU092291), and *P300* (EMU078861), and negative control (SIC001; Sigma) were ordered from Sigma. siRNA oligos were transfected into primary BMDMs using Lipofectamine 3000 (Invitrogen) following manufacturer's instructions.

Inhibitor treatment

Caspase inhibitor (Z-VAD (OMe)-FMK), caspase-1 inhibitor (Ac-YVAD-CMK), RIPK1 inhibitor (Necrostatin-1), RIPK3 inhibitor (GSK′872), and MLKL inhibitor (GW806742X) were purchased from MERCK and used for blocking cell death pathway. BMDMs were infected with *A. baumannii* in the presence or absence of various inhibitors for the indicated times.

LDH release assay

Cell culture supernatants were collected at the indicated times, and LDH activity was measured by using the Promega cytotoxicity kit according to the manufacturer's protocols.

ELISA

Cell culture supernatant was analyzed for cytokine release using ELISA kit (BioLegend ELISA MAX standard Billerica, MA) following the manufacturer's instructions.

Real-time quantitative PCR

Total RNA was isolated from BMDMs or liver and lung tissues using TRIzol (Invitrogen). cDNA was reverse transcribed by using M-MLV reverse transcriptase (Promega, Madison, USA). Real-time quantitative PCR was performed on the Bio-Rad CFX-96 Real-Time System. Primer sequences are listed in Table S1.

Statistical analysis

Data are given as mean ± s.e.m. Statistical analysis was performed using two-tailed Student's *t*-test, and log-rank tests. *P*-values ≤ 0.05 was considered significant.

Acknowledgements We thank Dr. Feng Shao for the *Ifnar*$^{-/-}$, *Irf3*$^{-/-}$/*Irf7*$^{-/-}$, and *Aim2*$^{-/-}$ mice, Dr. Shengzhong Duan (Shanghai Institutes for Biological Sciences, Chinese Academy of Sciences) for L929 cells, groups of Drs. Jumin Zhou, Yongtang Zheng, Jiali Li (Kunming Institute of Zoology) for technical assistance. This work was supported by the National Key Research and Development Program of China (2017YFD0500300), the Chinese Academy of Sciences (CXJJ-17-M141, Y4ZK111B01, QYZDJ-SSW-SMC012, and Y602381081), the National Natural Science Foundation of China (31701134 and 81701578), Chinese Academy Chinese National Natural Science Foundation (21761142002) and Key Laboratory of Bioactive Peptides of Yunnan Province (AMHD-2018-2).

Author contributions X. Qi designed the study; Y. Li, X. Guo, C. Hu, Y. Du, C. Guo, D. Wang, W. Zhao, G. Huang, C. Li, Q. Lu, R. Lai, T. Xu, and X. Qi performed experiments and analyzed the data; and X. Qi wrote the manuscript.

Compliance with Ethical Standards

Conflict of interest The authors declare that they have no conflict of interest.

References

1. Manchanda V, Sanchaita S, Singh NP, Multidrug resistant acinetobacter. J Glob Infect Dis. 2010;2:291–304.
2. Perez F, Hujer AM, Hujer KM, Decker BK, Rather PN, Bonomo RA, Global challenge of multidrug-resistant *Acinetobacter baumannii*. Antimicrob Agents Chemother. 2007;51:3471–84.
3. Eliopoulos GM, Maragakis LL, Perl TM, *Acinetobacter baumannii*: epidemiology, antimicrobial resistance, and treatment options. Clin Infect Dis. 2008;46:1254–63.
4. Ivashkiv LB, Donlin LT, Regulation of type I interferon responses. Nat Rev Immunol. 2014;14:36–49.
5. Carrero JA, Confounding roles for type I interferons during bacterial and viral pathogenesis. Int Immunol. 2013;25:663–9.
6. McNab F, Mayer-Barber K, Sher A, Wack A, O'Garra A, Type I interferons in infectious disease. Nat Rev Immunol. 2015;15:87–103.
7. Trinchieri G, Type I interferon: friend or foe?. J Exp Med. 2010;207:2053–63.
8. Gratz N, Hartweger H, Matt U, Kratochvill F, Janos M, Sigel S, et al. Type I interferon production induced by *Streptococcus pyogenes*-derived nucleic acids is required for host protection. PLoS Pathog. 2011;7:e1001345
9. Watanabe T, Asano N, Fichtner-Feigl S, Gorelick PL, Tsuji Y, Matsumoto Y, et al. NOD1 contributes to mouse host defense against *Helicobacter pylori* via induction of type I IFN and activation of the ISGF3 signaling pathway. J Clin Invest. 2010;120:1645–62.
10. de Almeida LA, Carvalho NB, Oliveira FS, Lacerda TLS, Vasconcelos AC, Nogueira L, et al. MyD88 and STING

signaling pathways are required for IRF3-mediated IFN-β induction in response to *Brucella abortus* infection. PLoS One. 2011;6: e23135
11. Henry T, Kirimanjeswara GS, Ruby T, Jones JW, Peng K, Perret M, et al. Type I IFN signaling constrains IL-17A/F secretion by γδ T cells during bacterial infections. J Immunol. 2010;184:3755–67.
12. Robinson N, McComb S, Mulligan R, Dudani R, Krishnan L, Sad S, Type I interferon induces necroptosis in macrophages during infection with Salmonella enterica serovar Typhimurium. Nat Immunol. 2012;13:954–62.
13. Stifter SA, Coleman MC, Feng CG. Regulation of host response to mycobacteria by type I interferons. In: Parker D, editor. Bacterial activation of type I interferons. Cham: Springer International Publishing;, 2014. p. 109–24.
14. O'Connell RM, Saha SK, Vaidya SA, Bruhn KW, Miranda GA, Zarnegar B, et al. Type I interferon production enhances susceptibility to *Listeria monocytogenes* infection. J Exp Med. 2004;200:437–45.
15. Chan FK-M, Luz NF, Moriwaki K. Programmed necrosis in the cross talk of cell death and inflammation. Annu Rev Immunol. 2015;33:79–106.
16. Bergsbaken T, Fink SL, Cookson BT, Pyroptosis: host cell death and inflammation. Nat Rev Microbiol. 2009;7:99–109.
17. Man SM, Karki R, Malireddi RKS, Neale G, Vogel P, Yamamoto M, et al. The transcription factor IRF1 and guanylate-binding proteins target activation of the AIM2 inflammasome by Francisella infection. Nat Immunol. 2015;16:467–75.
18. Rathinam Vijay AK, Vanaja Sivapriya K, Waggoner L, Sokolovska A, Becker C, Stuart Lynda M, et al. TRIF licenses caspase-11-dependent NLRP3 inflammasome activation by Gram-negative bacteria. Cell. 2012;150:606–19.
19. Carrero JA, Calderon B, Unanue ER, Type I interferon sensitizes lymphocytes to apoptosis and reduces resistance to Listeria infection. J Exp Med. 2004;200:535–40.
20. Qi X, Man SM, Malireddi RKS, Karki R, Lupfer C, Gurung P, et al. Cathepsin B modulates lysosomal biogenesis and host defense against *Francisella novicida* infection. J Exp Med. 2016;213:2081–97.
21. Murphy James M, Czabotar Peter E, Hildebrand Joanne M, Lucet Isabelle S, Zhang J-G, Alvarez-Diaz S, et al. The pseudokinase MLKL mediates necroptosis via a molecular switch mechanism. Immunity. 2013;39:443–53.
22. Chawla-Sarkar M, Lindner DJ, Liu YF, Williams BR, Sen GC, Silverman RH, et al. Apoptosis and interferons: role of interferon-stimulated genes as mediators of apoptosis. Apoptosis. 2003;8:237–49.
23. Henry T, Brotcke A, Weiss DS, Thompson LJ, Monack DM, Type I interferon signaling is required for activation of the inflammasome during Francisella infection. J Exp Med. 2007;204:987–94.
24. Gurung P, Malireddi RKS, Anand PK, Demon D, Walle LV, Liu Z, et al. Toll or interleukin-1 receptor (TIR) domain-containing adaptor inducing interferon-β (TRIF)-mediated caspase-11 protease production integrates toll-like receptor 4 (TLR4) protein- and Nlrp3 inflammasome-mediated host defense against enteropathogens. J Biol Chem. 2012;287:34474–83.
25. Storek KM, Gertsvolf NA, Ohlson MB, Monack DM, cGAS and Ifi204 cooperate to produce type I IFNs in response to Francisella infection. J Immunol. 2015;194:3236–45.
26. Kang M-J, Jo S-G, Kim D-J, Park J-H. NLRP3 inflammasome mediates interleukin-1β production in immune cells in response to *Acinetobacter baumannii* and contributes to pulmonary inflammation in mice. Immunology. 2017;150: 495-505.
27. Takaoka A, Wang Z, Choi MK, Yanai H, Negishi H, Ban T, et al. DAI (DLM-1/ZBP1) is a cytosolic DNA sensor and an activator of innate immune response. Nature. 2007;448:501–5.
28. Upton Jason W, Kaiser William J, Mocarski Edward S, DAI/ZBP1/DLM-1 complexes with RIP3 to mediate virus-induced programmed necrosis that is targeted by murine cytomegalovirus vIRA. Cell Host Microbe. 2012;11:290–7.
29. Kuriakose T, Man SM, Malireddi RKS, Karki R, Kesavardhana S, Place DE, et al. ZBP1/DAI is an innate sensor of influenza virus triggering the NLRP3 inflammasome and programmed cell death pathways. Sci Immunol. 2016;1:aag2045
30. Lin J, Kumari S, Kim C, Van T-M, Wachsmuth L, Polykratis A, et al. RIPK1 counteracts ZBP1-mediated necroptosis to inhibit inflammation. Nature. 2016;540:124–8.
31. Newton K, Wickliffe KE, Maltzman A, Dugger DL, Strasser A, Pham VC, et al. RIPK1 inhibits ZBP1-driven necroptosis during development. Nature. 2016;540:129–33.
32. Shi J, Zhao Y, Wang K, Shi X, Wang Y, Huang H, et al. Cleavage of GSDMD by inflammatory caspases determines pyroptotic cell death. Nature. 2015;526:660–5.
33. Ding J, Wang K, Liu W, She Y, Sun Q, Shi J, et al. Pore-forming activity and structural autoinhibition of the gasdermin family. Nature. 2016;535:111–6.
34. Qi X, Formation of membrane pores by gasdermin-N causes pyroptosis. Sci China Life Sci. 2016;59:1071–3.
35. Shi J, Gao W, Shao F. Pyroptosis: gasdermin-mediated programmed necrotic cell death. Trends Biochem Sci 2017; 42:245–254.
36. Schneider WM, Chevillotte MD, Rice CM. Interferon-stimulated genes: a complex web of host defenses. Annu Rev Immunol. 2014;32:513–45.
37. Bierne H, Hamon M, Cossart P, Epigenetics and bacterial infections. Cold Spring Harb Perspect Med. 2012;2:a010272
38. Saeed S, Quintin J, Kerstens HHD, Rao NA, Aghajanirefah A, Matarese F, et al. Epigenetic programming during monocyte to macrophage differentiation and trained innate immunity. Science. 2014;345:1251086.
39. Yue F, Cheng Y, Breschi A, Vierstra J, Wu W, Ryba T, et al. A comparative encyclopedia of DNA elements in the mouse genome. Nature. 2014;515:355–64.
40. Pasini D, Malatesta M, Jung HR, Walfridsson J, Willer A, Olsson L, et al. Characterization of an antagonistic switch between histone H3 lysine 27 methylation and acetylation in the transcriptional regulation of Polycomb group target genes. Nucleic Acids Res. 2010;38:4958–69.
41. Allis CD, Berger SL, Cote J, Dent S, Jenuwien T, Kouzarides T, et al. New nomenclature for chromatin-modifying enzymes. Cell. 2007;131:633–6.
42. Margueron R, Reinberg D, The polycomb complex PRC2 and its mark in life. Nature. 2011;469:343–9.
43. Tie F, Banerjee R, Conrad PA, Scacheri PC, Harte PJ, Histone demethylase UTX and chromatin remodeler BRM bind directly to CBP and modulate acetylation of histone H3 lysine 27. Mol Cell Biol. 2012;32:2323–34.
44. Kayagaki N, Stowe IB, Lee BL, O/'Rourke K, Anderson K, Warming S, et al. Caspase-11 cleaves gasdermin D for non-canonical inflammasome signalling. Nature. 2015;526: 666–71.
45. Shi J, Zhao Y, Wang Y, Gao W, Ding J, Li P, et al. Inflammatory caspases are innate immune receptors for intracellular LPS. Nature. 2014;514:187–92.
46. Kayagaki N, Wong MT, Stowe IB, Ramani SR, Gonzalez LC, Akashi-Takamura S, et al. Noncanonical inflammasome activation by intracellular LPS independent of TLR4. Science. 2013; 341:1246–9.

47. McComb S, Cessford E, Alturki NA, Joseph J, Shutinoski B, Startek JB, et al. Type-I interferon signaling through ISGF3 complex is required for sustained Rip3 activation and necroptosis in macrophages. Proc Natl Acad Sci. 2014;111: E3206–E3213.
48. Ge J, Gong Y-N, Xu Y, Shao F, Preventing bacterial DNA release and absent in melanoma 2 inflammasome activation by a *Legionella effector* functioning in membrane trafficking. Proc Natl Acad Sci USA. 2012;109:6193–8.
49. Guo C, Xie S, Chi Z, Zhang J, Liu Y, Zhang L, et al. Bile acids control inflammation and metabolic disorder through inhibition of NLRP3 inflammasome. Immunity. 2016;45:802–16.
50. Javed N, Xue G, Lu A, Xing Y, Iwakura Y, Xiao H, et al. Cross reactivity of S. aureus to murine cytokine assays: a source of discrepancy. Cytokine. 2016;81:101–8.
51. Qi X, Hong J, Chaves L, Zhuang Y, Chen Y, Wang D, et al. Antagonistic regulation by the transcription factors C/EBPa and MITF specifies basophil and mast cell fates. Immunity. 2013;39:97–110.